

# Reaction-diffusion processes and meta-population models in heterogeneous networks

Vittoria Colizza<sup>1,2\*</sup>, Romualdo Pastor-Satorras<sup>3</sup>, Alessandro Vespignani<sup>1,2</sup>

November 26, 2024

<sup>1</sup>Complex Networks Lagrange Laboratory, Institute for Scientific Interchange (ISI), Torino, Italy

<sup>2</sup>School of Informatics and Department of Physics, Indiana University, Bloomington 47406 IN

<sup>3</sup>Departament de Física i Enginyeria Nuclear, Universitat Politècnica de Catalunya, Campus Nord B4, 08034 Barcelona, Spain

\*e-mail: vcolizza@indiana.edu

**Dynamical reaction-diffusion processes and meta-population models are standard modeling approaches for a wide variety of phenomena in which local quantities – such as density, potential and particles – diffuse and interact according to the physical laws. Here, we study the behavior of two basic reaction-diffusion processes ( $B \rightarrow A$  and  $A + B \rightarrow 2B$ ) defined on networks with heterogeneous topology and no limit on the nodes' occupation number. We investigate the effect of network topology on the basic properties of the system's phase diagram and find that the network heterogeneity sustains the reaction activity even in the limit of a vanishing density of particles, eventually suppressing the critical point in density driven phase transitions, whereas phase transition and critical points, independent of the particle density, are not altered by topological fluctuations. This work lays out a theoretical and computational microscopic framework for the study of a wide range of realistic meta-populations models and agent-based models that include the complex features of real world networks.**

Reaction-diffusion (RD) processes are used to model phenomena as diverse as chemical reactions, population evolution, epidemic spreading and many other spatially distributed systems in which local quantities obey physical reaction diffusion equations<sup>1,2,3</sup>. At the microscopic level, RD processes generally consist of particles (in many cases accounting for different kinds of “agents”, information parcels, etc.) that diffuse in space and are subject to various reaction processes determined by the nature of the specific problem at hand. While fermionic RD models assume exclusion principles that limit the number of particles on each node of the lattice, bosonic RD processes relax these constraints and allow each node of the lattice to be occupied by any number of particles. The classic example is provided by chemical reactions, in which different molecules or atoms diffuse in space and may react whenever in close contact. Another important instance for bosonic RD processes is found in meta-population epidemic models<sup>4,5,6,7,8,9,10</sup>. In this case particles represent people moving between different locations, such as cities or urban areas. Individuals are divided into classes denoting their state with respect to the modeled disease—such as infected, susceptible, immune, etc.—and the reaction processes account for the possibility that individuals in the same location may get in contact and change their state according to the infection dynamics.

The above modeling approaches are based on the spatial structure of the environment, transportation infrastructures, movement patterns, traffic networks, etc. The lack of accurate data on those features of the systems were usually reflected in the use of random graphs and regular lattices of different dimensionality as the substrate of the RD process. This corresponds to an implicit homogeneous assumption on the structure of the substrate, indeed used in many instances to solve the basic equations describing the RD process. In recent years, however, networks which trace the activities and interactions of individuals, social patterns, transportation fluxes, and population movements on a local and global scale<sup>11,12,13,14,15</sup> have been analyzed and found to exhibit complex features encoded in large scale heterogeneity, self-organization and other properties typical of complex systems<sup>16,17,18,19</sup>. In particular it has been found that a

wide range of societal and technological networks exhibit a very heterogeneous topology. The airport network among cities<sup>13,14</sup>, the commuting patterns in inter and intra-urban areas<sup>15,20</sup>, and several info-structures<sup>19</sup> are indeed characterized by networks whose nodes, representing the elements of the system, have a wildly varying degree, i.e. the number of connections to other elements. These topological fluctuations are mathematically encoded in a heavy-tailed degree distribution  $P(k)$ , defined as the probability that any given node has degree  $k$ . They thus define highly heterogeneous substrates for the RD processes that cannot be accounted for in homogeneous or translationally invariant lattices. Analogously, models aimed at a description of spreading processes in spatially extended and societal systems are inevitably occurring in meta-population networks with connectivity patterns displaying very large fluctuations. Since connectivity fluctuations have been shown to have a large impact on the behavior of several percolation and fermionic systems<sup>21,22,23</sup>, the investigation of their role in the case of bosonic RD processes becomes a crucial issue for the understanding of a wide array of real world phenomena.

### **Reaction-diffusion processes in complex networks.**

In order to investigate the effect of network heterogeneities on the phase diagram of meta-population models and chemical reaction processes, we consider a basic reaction scheme conserving the number of particles that has been studied both in physics and mathematical epidemiology, namely the reaction-diffusion process identified by the following set of reactions<sup>1,24,25,26,27,28</sup>:



From these reaction equations it is clear that the dynamics conserves the total number of particles  $N = N_A + N_B$ , where  $N_i$  is the number of particles  $i = A, B$ . This process can be naturally interpreted as a chemical reaction with an absorbing state phase transition<sup>1,25,26</sup>. The same reaction has been however used as a model problem in population dynamics in interaction with a polluting substance<sup>27</sup>, and it is analogous to the classic susceptible-infected-susceptible

(SIS) model for epidemic spreading<sup>4,28</sup>. In the process described by eqs. (1)-(2) the dynamics is exclusively due to  $B$  particles, that we identify as *active* particles, since  $A$  particles cannot generate spontaneously  $B$  particles. We consider the particles diffusing on a heterogeneous network with  $V$  nodes having a degree distribution  $P(k)$  characterized by the first and second moments  $\langle k \rangle$  and  $\langle k^2 \rangle$ , respectively. Reaction processes take place inside the network's nodes only, where each node  $i$  stores a number  $a_i$  of  $A$  particles and  $b_i$  of  $B$  particles (see Figure 1). The occupation numbers  $a_i$  and  $b_i$  can assume any integer value, including  $a_i = b_i = 0$ , that is, void nodes with no particles. For the sake of simplicity we assume that  $B$  particles diffuse with unitary time rate  $D_B = 1$  along one of the links departing from the node in which they are at a given time. This implies that at each time step a particle sitting on a node with degree  $k$  will jump into one of its nearest neighbor with probability  $1/k$ . The results obtained in the following may be recovered for any diffusion rate  $D_B$ , at the expense of a more complicate mathematical treatment that will be reported elsewhere. In the case of  $A$  particles, we consider two different situations corresponding to a unitary ( $D_A = 1$ ) and a null ( $D_A = 0$ ) diffusion rate, respectively. While the first case is used in epidemic models which consider all individuals diffusing with the same rate, the case  $D_A = 0$  is used in self-organized critical systems and specific absorbing phase transitions coupled with non-diffusive fields<sup>28,25,26</sup>. When  $D_A = 0$ , the diffusion of  $A$  particles in the network occurs only through an effective process mediated by the reaction with  $B$  particles. Indeed any  $A$  particle may become a  $B$  particle following the reaction process and diffuse in the network until the reaction  $B \rightarrow A$  occurs. This process is thus equivalent to an effective diffusion of  $A$  particles in the network.

Before the diffusion process, the  $a_i$  and  $b_i$  particles stored in the same node react according to eqs. (1) and (2). In each node  $i$  the spontaneous process  $B \rightarrow A$  simply consists in turning each  $b_i$  particle into an  $a_i$  particle with rate  $\mu$ . We consider two general forms for the  $B + A \rightarrow 2B$  process. In *type I* reaction we consider that each  $a_i$  may react with all the  $b_i$  particles in the same node, each reaction occurring with rate  $\beta$ . In *type II* reaction we consider instead that each particle has a finite number of contacts with other particles. In this case the reaction

rate has to be rescaled by the total number of particles present in the node, i.e.  $\beta/\rho_i$ , where  $\rho_i = a_i + b_i$  is the total number of particles in the node. This second process corresponds to what we usually observe in epidemic processes, where there is a population dependence of the reaction rate since individuals generally meet with a definite number of other individuals. In regular lattices and within the homogeneous mixing (mean-field) hypothesis, both type of processes exhibit a phase transition from an active phase (with an everlasting activity of B particles) to an absorbing phase (devoid of B particles), which in epidemic modeling correspond to the infected and healthy states, respectively. In the type I reaction the relevant parameter is represented by the average density of particles  $\rho = N/V$  and the transition occurs at the threshold value  $\rho = \rho_c = \mu/\beta$ <sup>25,26,28</sup>. In the type II processes the transition point is found whenever  $\beta/\mu > 1$ . This second case is analogous to the classical epidemic threshold result and determines the lack or existence of an endemic state with a finite density of infected individuals (in this representation corresponding to the B particles)<sup>3,4</sup>.

In order to take into account the topological fluctuations of the networks we have to explicitly consider the presence of nodes with very different degree  $k$ . A convenient representation of the system is therefore provided by the quantities

$$\rho_{A,k} = \frac{1}{v_k} \sum_{i|k_i=k} a_i, \quad \rho_{B,k} = \frac{1}{v_k} \sum_{i|k_i=k} b_i, \quad (3)$$

where  $v_k$  is the number of nodes with degree  $k$  and the sums run over all nodes  $i$  having degree  $k_i$  equal to  $k$ . These two quantities express the average number of A and B particles in nodes with degree  $k$ . Analogously,  $\rho_k = \rho_{A,k} + \rho_{B,k}$  represents the average number of particles in nodes with degree  $k$ . The average density of A and B particles in the network is given by  $\rho_A = \sum_k P(k)\rho_{A,k}$  and  $\rho_B = \sum_k P(k)\rho_{B,k}$ , respectively. Finally, by definition it follows that  $\rho = \rho_A + \rho_B$ . These quantities allow to express the RD process occurring on a heterogeneous network in terms of a set of rate equations describing the time evolution of the quantities  $\rho_{A,k}(t)$  and  $\rho_{B,k}(t)$  for each degree class  $k$ , as reported in the Materials and Methods section. The equations depend on the reaction kernel  $\Gamma_k$  that yields the number of B particles generated per unit time by the reaction processes taking place in nodes of a given degree class  $k$ . In uncorrelated

networks the resulting equations can be solved in the stationary limit, thus providing information on the phase diagram of the processes.

### Phase diagram and critical threshold.

Let us first consider the type I reaction processes in uncorrelated networks. In this case we have that  $\Gamma_k = \rho_{A,k}\rho_{B,k}$  obtaining in the stationary state

$$\rho_{B,k} = \frac{k}{\langle k \rangle} [(1 - \mu)\rho_B + \beta\Gamma], \quad (4)$$

where  $\Gamma = \sum_k P(k)\Gamma_k$ . This equation readily states that the density of active particles is increasing in nodes with increasing degree  $k$ . This effect is mainly due to the diffusion process, that brings a large number of particles to well connected nodes, reflecting thus the impact of the network topological fluctuations on the particle density behavior (see the online supplementary information). In order to study the phase diagram we have to find the condition for which a solution  $\rho_B \neq 0$  of the set of equations for  $\rho_{A,k}(t)$  and  $\rho_{B,k}(t)$  is allowed. If  $D_A = 0$ , i.e. for the case of non diffusing  $A$  particles, the density of  $A$  particles is independent of the node degree and is given by  $\rho_{A,k} = \rho_A = \mu/\beta$ . In view of the conservation of the number of particles this result readily implies that  $\rho_B = \rho - \frac{\mu}{\beta}$  and therefore the presence of a phase transition from an absorbing phase to an active state at a critical value of the total density of particles  $\rho_c = \frac{\mu}{\beta}$ . A very different picture is obtained when  $A$  particles are also allowed to diffuse. In this case, for  $D_A = 1$ , the stationary density of  $A$  particles is given by

$$\rho_{A,k} = \frac{k}{\langle k \rangle} (\rho_A + \mu\rho_B - \beta\Gamma). \quad (5)$$

The system of equations can be solved by imposing a self-consistent condition for the quantity  $\Gamma$  (the details of the calculation are reported in the online supplementary information) and the non-trivial solution  $\rho_B > 0$  is obtained only if the total density of particles satisfies the condition  $\rho > \rho_c$ , with

$$\rho_c = \frac{\langle k \rangle^2 \mu}{\langle k^2 \rangle \beta}. \quad (6)$$

This result implies that, if  $A$  particles can diffuse, topological fluctuations affect the critical value of the transition. Networks characterized by heterogeneous connectivity patterns display large degree fluctuations so that  $\langle k^2 \rangle \gg \langle k \rangle^2$ . In the infinite size limit  $V \rightarrow \infty$  we have  $\langle k^2 \rangle \rightarrow \infty$  and thus eq. (6) yields a critical value  $\rho_c = 0$ , showing that the topological fluctuations of the network suppress the phase transition in the thermodynamic limit. This is a very relevant result that, analogously to those concerning percolation<sup>21,22</sup> and standard epidemic processes<sup>23</sup>, indicates that physical and dynamical processes taking place on scale-free and heavy-tailed networks behave very differently with respect to the same processes occurring on homogeneous networks.

In Figure 2 we provide support to this theoretical picture by reporting the results obtained from Monte Carlo simulations of RD processes of type I on uncorrelated networks with given scale-free degree distribution  $P(k) \sim k^{-\gamma}$ . The simulations use a single particle modeling strategy in which each individual particle is tracked in time. The system evolves following a stochastic microscopic dynamics and at each time step it is possible to record average quantities, such as e.g. the density of active particles  $\rho_B(t)$ . In addition, given the stochastic nature of the dynamics, the experiment can be repeated with different realizations of the noise, different underlying graphs, and different initial conditions. This approach is equivalent to the real evolution of the RD process in the generated networks and can be used to validate the theoretical results obtained in the analytical approach. The top panel of Figure 2 shows the phase transitions observed in the two cases, whether  $A$  particles diffuse or not. If  $D_A = 0$  the process undergoes a phase transition at  $\rho_c = \mu/\beta = 2$ , regardless of the difference in the level of heterogeneity as provided by different values of the power-law exponent  $\gamma$  of the degree distribution  $P(k)$  at fixed network size (here  $V = 10^4$ ,  $\gamma = 3$  and  $\gamma = 2.5$ ) or by different sizes  $V$  at fixed  $\gamma$  ( $\gamma = 2.5$ ,  $V = 10^4$  and  $V = 10^5$ ). In case  $A$  particles diffuse, instead, the transition occurs at critical values  $\rho_c < \mu/\beta$ , with  $\rho_c \rightarrow 0$  for decreasing ratios  $\langle k \rangle^2 / \langle k^2 \rangle$  as observed for increasing sizes  $V$  at fixed  $\gamma$  (curves for  $\gamma = 2.5$  with  $V$  from  $10^3$  to  $10^5$  nodes are shown), in agreement with the analytical result of eq. (6). Bottom panels show the difference in the behavior of  $\rho_{A,k}$

as a function of the degree  $k$ : a flat spectrum is obtained when  $D_A = 0$  and a linear dependence in  $k$  when  $D_A = 1$ .

A different scenario emerges when considering type II processes. In this case the reaction kernel is  $\Gamma_k = \rho_{A,k}\rho_{B,k}/\rho_k$ ; i.e. in each node  $A$  particles will participate in a reaction event with a rate proportional to the relative density of  $B$  particles. While the set of equations for  $\rho_{B,k}$  has the same form of eq. (4), the stationary condition for  $\rho_{A,k}$  yields solutions that depend on  $k$  for both diffusive and non-diffusive  $A$  particles. In particular, in both cases we have that  $\rho_B > 0$  if the condition  $\beta/\mu > 1$  is satisfied (see the online supplementary information). This result recovers the usual threshold condition which depends only on the reaction rates and is not affected by changes in the total density of particles  $\rho$ . Also for type II processes we performed extensive Monte-Carlo simulations considering uncorrelated scale-free networks with a heavy tailed degree distribution. Figure 3 reports the results obtained in the two cases  $D_A = 0$  and  $D_A = 1$ , with different underlying network topologies. Changes in the number of nodes and in the exponent  $\gamma$  assumed for the degree distribution do not affect the phase transition. The critical value depends exclusively on the process rates, despite the observed linear behavior of  $\rho_{A,k}$  and  $\rho_{B,k}$  bears memory of the heterogeneity of the underlying network.

### **Discussion and comparison with realistic models.**

The different phase diagrams obtained in type I and II processes can be understood qualitatively in terms of the following argument. In type I processes, whatever the parameters  $\beta$  and  $\mu$ , there exists a value of the local density large enough to keep the system in an active state by sustaining the creation of  $B$  particles in the right amount. Large topological fluctuations imply the existence of high degree nodes with a high density of particles and therefore a high number of generated  $B$  particles. This implies that in the thermodynamic limit there is always a node (with a virtually infinite degree) with enough particles to keep alive the process even for a vanishing average density of particles, leading to the suppression of the phase transition. The crucial ingredient of this mechanism is given by the diffusion process that allows high degree



nodes to have a number of particles that is proportional to their degree. This is confirmed by the case in which  $A$  particles do not diffuse. In this case high degree nodes do not accumulate enough particles and the usual threshold effect is recovered. In type II processes, on the other hand, the reaction activity in each node is rescaled by the local density  $\rho_i$  and it is therefore the same in all nodes, regardless of the local population. In this case, the generation of  $B$  particles is homogeneous across nodes of different degrees and therefore the presence of an active state depends only on the balance between the reaction rates  $\beta$  and  $\mu$ .

These results let emerge a basic framework for the microscopic (mechanistic in the epidemic terminology) description of meta-population epidemic models. The type I and II processes correspond to the two limits of transmissibility independent or inversely proportional to the population size, respectively. In addition, realistic meta-population models have heterogeneous diffusion probabilities due to the traveling pattern and fixed population sizes according to data. Despite these extra complications, the basic reaction-diffusion framework studied here provides a simple qualitative picture of the realistic models. In Figure 4 we report the two types of processes studied here and compare them with the results from a realistic compartmental SIS meta-population model considering 500 urban areas in the United States and including the actual data of the air traveling flows among those urban areas<sup>33,34</sup>. The network is defined by nodes representing each urban area together with its population and edges representing air travel fluxes along which individuals diffuse, coupling the epidemic spreading in different urban areas (see Ref.<sup>35,36,37</sup> for a detailed definition of the model). The type I process is compared with a model whose transmissibility is independent of the population size and the type II process is compared with the usual epidemic spreading with transmissibility scaling proportionally to the population size (see Ref.<sup>5</sup>). Figure 4 shows in the four cases the reaction activity occurring on each network node, i.e. the creation of  $B$  particles in the reaction-diffusion process and newly infected individuals in the realistic epidemic model normalized to the local population. Increasing values of the reaction activity correspond to colors ranging from yellow (low activity) to red (high activity). In type I processes the reaction activity is linearly increasing with the pop-

ulation of the nodes, thus showing high activity (red) concentrated in largely populated nodes (represented with a larger size). The homogeneity in the generation of B particles in type II processes is evident: all nodes display the same color and thus experience the same level of activity, regardless of the local density. Strikingly, despite the various complications and elements of realism introduced in the data-driven meta-population model, its qualitative behavior is in very good agreement with the results obtained for the microscopic reaction-diffusion processes in both transmissibility limits.

In summary, the microscopic RD framework introduced here is able to provide a general theoretical understanding of the behavior of more realistic meta-population epidemic models. Furthermore, the presented approach can be extended to include the various sources of heterogeneity—such as degree correlations<sup>29,30</sup>, heterogeneous diffusion probabilities and their non-linear relations with the connectivity pattern—needed in order to provide a detailed analysis of realistic processes.

## Materials and Methods

*Reaction-diffusion equation.* In order to take fully into account degree fluctuations in an analytical description of the RD processes, we have to relax the homogeneity assumption and allow for degree fluctuations by introducing the relative densities  $\rho_{B,k}(t)$ ,  $\rho_{A,k}(t)$ , and  $\rho_k(t)$ . The dynamical reaction rate equations for B particles in any given degree class can thus be written as

$$\partial_t \rho_{B,k} = -\rho_{B,k} + k \sum_{k'} P(k'|k) \frac{1}{k'} [(1 - \mu)\rho_{B,k'} + \beta\Gamma_{k'}], \quad (7)$$

where  $P(k'|k)$  represents the conditional probability that a vertex of degree  $k$  is connected to a vertex of degree  $k'$ <sup>29</sup>. The various terms of the equations are obtained by considering that at each time step the particles present on a node of degree  $k$  first react and then diffuse away from the node with unitary diffusion rate accounted by the term  $-\rho_{B,k}$ . The positive contribution for the particle density is obtained by summing the contribution of all particles diffusing in nodes of degree  $k$  from their neighbors of any degree  $k'$ , including the new particles generated by the

reaction term  $\Gamma_k$ . In the case of uncorrelated networks the conditional probability  $P(k'|k)$  that any given edge points to a vertex with  $k'$  edges is independent of  $k$  and equal to  $k'P(k')/\langle k \rangle$ <sup>18,29</sup>, so that the reaction rate equations read as

$$\partial_t \rho_{B,k} = -\rho_{B,k} + \frac{k}{\langle k \rangle} [(1 - \mu)\rho_B + \beta\Gamma], \quad (8)$$

where  $\rho_B = \sum_k P(k)\rho_{B,k}$  and  $\Gamma = \sum_k P(k)\Gamma_k$ . In the case for  $\rho_{A,k}(t)$  we have to distinguish whether if  $A$  particles diffuse or not. If  $D_A = 1$ , we obtain a set of equations analogous to those for  $\rho_{B,k}$  that read as

$$\partial_t \rho_{A,k} = -\rho_{A,k} + \frac{k}{\langle k \rangle} (\rho_A + \mu\rho_B - \beta\Gamma), \quad (9)$$

where  $\rho_A = \sum_k P(k)\rho_{A,k}$ . In the case of non-diffusive  $A$  particles ( $D_A = 0$ ) the equations reduce to:

$$\partial_t \rho_{A,k} = \mu\rho_{B,k} - \beta\Gamma_k. \quad (10)$$

The phase diagram for the various cases and the conditions for  $\rho_B > 0$  are obtained by imposing the stationary state defined by  $\partial_t \rho_{A,k} = 0$  and  $\partial_t \rho_{B,k} = 0$ , with the additional constraint that  $\rho = \rho_A + \rho_B$ , i.e. the number of particles is conserved. We are therefore led to a simple set of algebraic equations whose explicit solution is reported in the online supplementary information.

*Monte-Carlo simulations.* The uncorrelated networks considered have been generated with the *uncorrelated configuration model*<sup>31</sup>, based on the *Molloy-Reed*<sup>32</sup> algorithm with an additional constraint on the possible maximum value of the degree in order to avoid inherent structural correlations. The algorithm is defined as follows. Each node  $i$  is assigned a degree  $k_i$  obtained from a given degree sequence  $P(k)$  (in our case  $P(k) \sim k^{-\gamma}$  with  $\gamma = 3$  and  $\gamma = 2.5$ ) subject to the restriction  $k_i < V^{1/2}$ . Links are then drawn to randomly connect pairs of nodes, respecting their degree and avoiding self-loops and multiple edges. Sizes of  $V = 10^3$ ,  $V = 10^4$  and  $V = 10^5$  nodes have been considered. Initial conditions are generated by randomly placing  $V\rho_A(0)$  particles  $A$  and  $V\rho_B(0)$  particles  $B$ , corresponding to a particle density  $\rho = \rho_A(0) + \rho_B(0)$ . The results are independent of the particular initial ratio  $\rho_A(0)/\rho_B(0)$ , apart from very early time transients. The dynamics proceeds in parallel and considers discrete

time steps representing the unitary time scale  $\tau$  of the process. The reaction and diffusion rates are therefore converted into probabilities and at each time step, the system is updated according to the following rules. a) Reaction processes: *i*) On each lattice site, each  $B$  particle is turned into an  $A$  particle with probability  $\mu\tau$ . *ii*) At the same time, each  $A$  particle becomes a  $B$  particle with probability determined by the type of reaction process. b) After all nodes have been updated for the reaction, we perform the diffusion: on each lattice site, each  $B$  particle moves into a randomly chosen nearest neighbor site; the same process occurs for  $A$  particles if  $D_A = 1$ . The simulation details of the reaction process represented by eq. (2) depend on the kernel considered. In type I processes each  $A$  particle in a given node  $i$  becomes a  $B$  particle with probability  $1 - (1 - \beta\tau)^{b_i}$ , where  $b_i$  is the total number of  $B$  particles in that node. This corresponds to the average probability for an  $A$  particle of being involved in the reaction (2) with any of the  $B$  particles present on the same site. In type II processes the reaction process is simulated by turning each  $A$  particle into a  $B$  particle with probability  $1 - (1 - \frac{\beta}{\rho_i}\tau)^{b_i}$  where  $\rho_i$  is the total number of particles in the node  $i$ . This term accounts for the average probability that an  $A$  particle will get in contact with a  $B$  particle present in the node, given that the possible number of contacts is rescaled by the population  $\rho_i$  of the node. The term  $\beta/\rho_i$  therefore represents the normalized transmission rate of the process.

Correspondence and requests for material should be addressed to V.C. (vcolizza@indiana.edu) or A.V. (alexv@indiana.edu).

**Acknowledgments** A.V. is partially supported by the NSF award IIS-0513650. R. P.-S. acknowledges financial support from the Spanish MEC (FEDER), under project No. FIS2004-05923-C02-01 and additional support from the DURSI, Generalitat de Catalunya (Spain).

## References

1. Marro, J. & Dickman, R. *Nonequilibrium Phase Transitions in Lattice Models* (Cambridge University Press, Cambridge, England, 1999).
2. van Kampen, N.G. *Stochastic processes in chemistry and physics* (North Holland, Amsterdam, 1981).
3. Murray, J.D. *Mathematical Biology* (Springer–Verlag Berlin, Heidelberg, 3rd edition 2005).
4. Anderson, R.M. & May, R.M. *Infectious Diseases of Humans: Dynamics and Control* (Oxford University Press, Oxford, 1992).
5. Anderson, R.M. & May, R.M. Spatial heterogeneity and the design of immunization programs. *Math Biosciences*, **72**, 83–111 (1984).
6. Bolker, B.M. & Grenfell, B.T. Space persistence and dynamics of measles epidemics. *Phil. Trans. R. Soc. Lond.* **B348**, 309–320 (1995).
7. Lloyd, A.L. & May, R.M. Spatial heterogeneity in epidemic models. *J. Theor. Biol.*, **179**, 1–11 (1996).
8. Grenfell, B.T. & Bolker, B.M. Cities and villages: infection hierarchies in a measles metapopulation. *Ecology Letters*, **1**, 63–70 (1998).
9. Keeling, M.J. & Rohani, P. Estimating spatial coupling in epidemiological systems: a mechanistic approach. *Ecology Letters*, **5**, 20–29 (1995).
10. Ferguson, N.M., Keeling, M.J., Edmunds, W.K., Gani, R., Grenfell, B.T., Anderson, R.M., & Leach, S. Planning for smallpox outbreaks. *Nature* **425**, 681–685 (2003).
11. Liljeros, F., Edling, C.R., Amaral, L.A.N., Stanley, H.E., & Aberg, Y. The web of human sexual contacts. *Nature* **411**, 907–908 (2001).

12. Schneeberger, A., Mercer, C.H., Gregson, S.A., Ferguson, N.M., Nyamukapa, C.A., Anderson, R.M., Johnson, A.M., & Garnett, G.P. Scale-free networks and sexually transmitted diseases: a description of observed patterns of sexual contacts in Britain and Zimbabwe. *Sexually Transmitted Diseases* **31**, 380–387 (2004).
13. Barrat, A., Barthélemy, M., Pastor-Satorras, R. & Vespignani, A. The architecture of complex weighted networks. *Proc. Natl. Acad. Sci. USA* **101**, 3747–3752 (2004).
14. Guimerà, R., Mossa, S., Turtschi, A. & Amaral, L.A.N. The worldwide air transportation network: Anomalous centrality, community structure, and cities' global roles. *Proc. Natl. Acad. Sci. USA* **102**, 7794–7799 (2005).
15. Chowell, G., Hyman, J.M., Eubank, S. Castillo-Chavez, C. Scaling Laws for the movement of people between locations in a large city. *Phys. Rev. E* **68**, 066102 (2003).
16. Albert, R. & Barabási, A.-L. Statistical mechanics of complex networks. *Rev. Mod. Phys.* **74**, 47–97 (2002).
17. Newman, M.E.J. The Structure and Function of Complex Networks. *SIAM Review* **45**, 167–256 (2003).
18. Dorogovtsev, S.N. & Mendes, J.F.F. *Evolution of networks: From Biological nets to the Internet and WWW* (Oxford Univ. Press, Oxford, 2003).
19. Pastor-Satorras, R. & Vespignani, A. *Evolution and Structure of the Internet: A statistical physics approach* (Cambridge Univ. Press, Cambridge, 2004).
20. Barrett, C.L. *et al.*, TRANSIMS: Transportation Analysis Simulation System (Technical Report LA-UR-00-1725, Los Alamos National Laboratory, 2000).
21. Cohen, R., Erez, K., ben-Avraham, D., & Havlin, S. Resilience of the Internet to random breakdowns. *Phys. Rev. Lett.* **85**, 4626–4628 (2000).

22. Callaway, D. S., Newman, M. E. J., Strogatz, S., H. & Watts, D. J. Network robustness and fragility: percolation on random graphs. *Phys. Rev. Lett.* **85**, 5468–5471 (2000).
23. Pastor-Satorras, R., & Vespignani, A. Epidemic spreading in scale-free networks. *Phys. Rev. Lett.* **86**, 3200–3203 (2001).
24. Cardy, J.L., & Grassberger P. Epidemics models and percolation. *Journal of Physics A* **18**, L267–L271 (1985).
25. de Freitas, J.E., Lucena, L.S., da Silva, L.R., & Hilhorst, H.J. Critical behavior of a two-species reaction-diffusion problem. *Phys. Rev. E* **61**, 6330–6336 (2000).
26. Pastor-Satorras, R., & Vespignani, A. Field theory of absorbing phase transitions with a nondiffusive conserved field. *Phys. Rev. E* **62** R5875–R5878 (2000).
27. Kree, R., Schaub, B. & Schmittman, B. Effects of pollution on critical population dynamics. *Phys. Rev. A* **39**, 2214–2221 (1989).
28. van Wijland, F., Oerding, K., & Hilhorst, H.J. Wilson renormalization of a reaction-diffusion process. *Physica A* **251**, 179–201 (1998).
29. Pastor-Satorras, R., Vázquez, A. & Vespignani, A. Dynamical and Correlation Properties of the Internet. *Phys. Rev. Lett.* **87**, 258701 (2001).
30. Newman, M.E.J., Assortative Mixing in Networks. *Phys. Rev. Lett.* **89**, 208701 (2002).
31. Catanzaro, M., Boguna, M., Pastor-Satorras, R. Generation of uncorrelated random scale-free networks. *Phys. Rev. E* **71**, 027103 (2005).
32. Molloy, M. & Reed, B., A critical point for random graphs with a given degree sequence. *Random Structures Algorithms* **6**, 161–179 (1995).
33. International Air Transport Association (IATA). <http://www.iata.org/>.

- 
34. US Census Bureau. <http://www.census.gov/>.
  35. Rvachev, L.A. & Longini, I.M., A mathematical model for the global spread of influenza. *Math. Biosci.* **75**, 3–22 (1985).
  36. Hufnagel, L., Brockmann, D. & Geisel, T., Forecast and control of epidemics in a globalized world. *Proc. Natl. Acad. Sci. USA* **101**, 15124–15129 (2004).
  37. Colizza, V., Barrat, A., Barthélemy, M. & Vespignani, A., The role of the airline transportation network in the prediction and predictability of global epidemics. *Proc. Natl. Acad. Sci. USA* **103**, 2015–2020 (2006).



## Figure captions

**Figure 1. Bosonic reaction-diffusion systems in heterogeneous networks.** Schematic representation of RD processes in heterogeneous complex networks when the multiple occupancy of nodes is allowed. Particles  $A$  and  $B$  can diffuse in the network and, inside each node, undergo the reaction processes described by eqs. (1)–(2). Each node  $i$  stores  $\rho_i = a_i + b_i$  particles, where the occupation numbers  $a_i$  and  $b_i$  can assume any integer value, including zero.

**Figure 2. Phase diagram and stationary densities for type I processes.** Top panel: Phase transitions in type I processes for diffusing and non-diffusing  $A$  particles. If  $D_A = 0$  the transition occurs at the critical value of the density  $\rho_c = \mu/\beta = 2$ , regardless of the topology of the underlying network. Results for uncorrelated scale-free networks having degree distribution  $P(k) \sim k^{-\gamma}$  with  $\gamma = 2.5$  and  $\gamma = 3.0$  and different sizes  $V$  show the same behavior, small differences in the value of  $\rho_B$  being due to finite-size effects. If  $D_A = 1$ , the critical point is strongly affected by the topological fluctuations of the network. Here we show results for  $\gamma = 2.5$  and sizes of the network  $V = 10^3, 10^4, 10^5$  corresponding to  $\langle k \rangle^2 / \langle k^2 \rangle = 0.52, 0.32, 0.19$ , respectively. With increasing sizes, degree fluctuations become larger and the transition is observed at smaller values of  $\rho_c$ . Bottom panels: Stationary densities  $\rho_{A,k}$  and  $\rho_{B,k}$  as functions of the degree  $k$ . If  $D_A = 0$ , the average density of  $A$  particles inside nodes of degree  $k$  is constant, while the behavior shown by  $B$  particles is linear in  $k$ . If  $D_A = 1$ , both densities are linear in  $k$ .

**Figure 3. Phase diagram and stationary densities for type II processes.** Top panel: Phase transitions in type II processes for diffusing and non-diffusing  $A$  particles. Regardless of topological fluctuations in the underlying network and of the probability of diffusion  $D_A$ , the transition occurs at the critical point  $\beta/\mu = 1$ , depending only on the reaction rates. Here we show results for networks of size  $V = 10^4$  with particle density  $\rho = 20$ , power-law exponents  $\gamma = 2.5$

and  $\gamma = 3.0$ . Differences in the values of the stationary density  $\rho_B$  are due to finite-size effects. Bottom panels: Stationary densities  $\rho_{A,k}$  and  $\rho_{B,k}$  as functions of the degree  $k$ . In both cases,  $D_A = 0$  and  $D_A = 1$ , linear dependencies in  $k$  are obtained.

**Figure 4. Reaction activity in type I and type II processes: microscopic model and real-world examples.** The first row of panels refers to the microscopic RD model, as described in the text, while the second row reports the analysis of the spread of an airline-carried disease in the US with a data-driven meta-population model. Both models consider the actual topology of the US air transportation network as obtained by considering the 500 airports with largest traffic<sup>33</sup>; nodes population is obtained from census data<sup>34</sup>. In addition, the realistic meta-population model also considers the actual traffic of passengers on each connection between airports. The networks are mapped on a globe for sake of visualization. Each node is represented with a size linearly dependent on its population and a color illustrating the level of reaction activity inside the node, ranging from 0 to the max value. Whereas type I processes experience a level of activity proportional to nodes population – corresponding to red color in largely populated nodes and yellow in small population nodes – the reaction activity is homogeneously distributed among the nodes of the network when type II processes are considered.

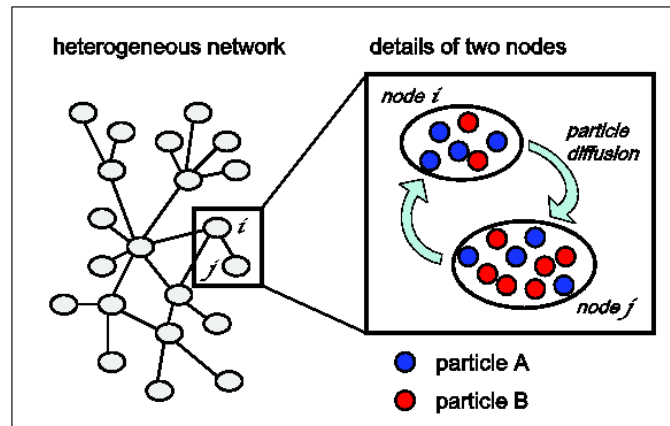


Figure 1.

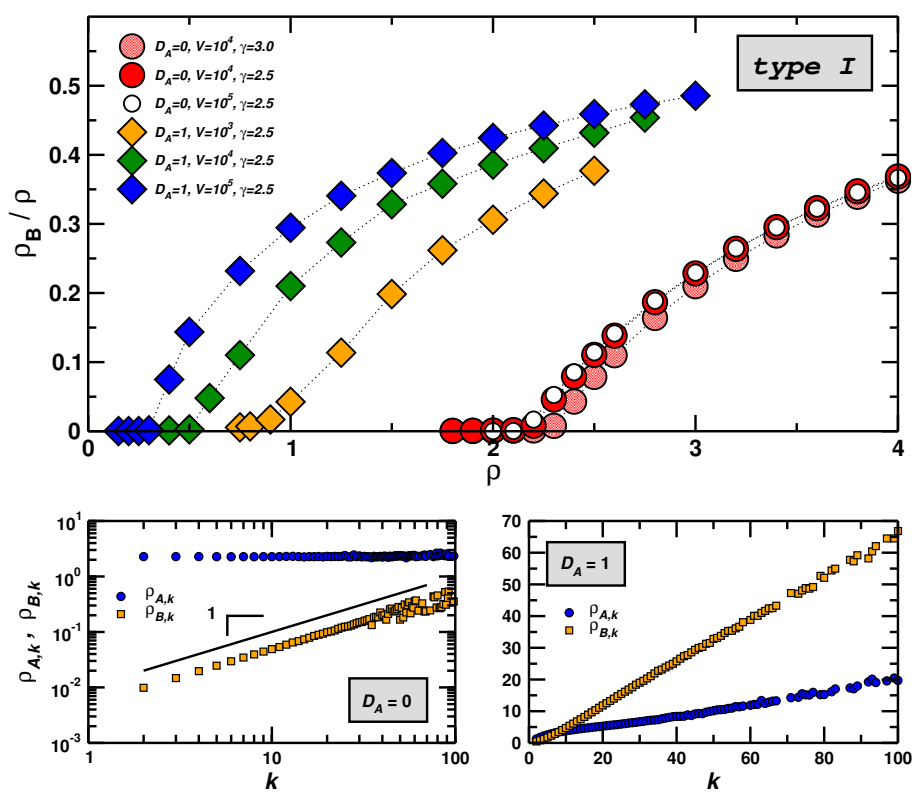


Figure 2.

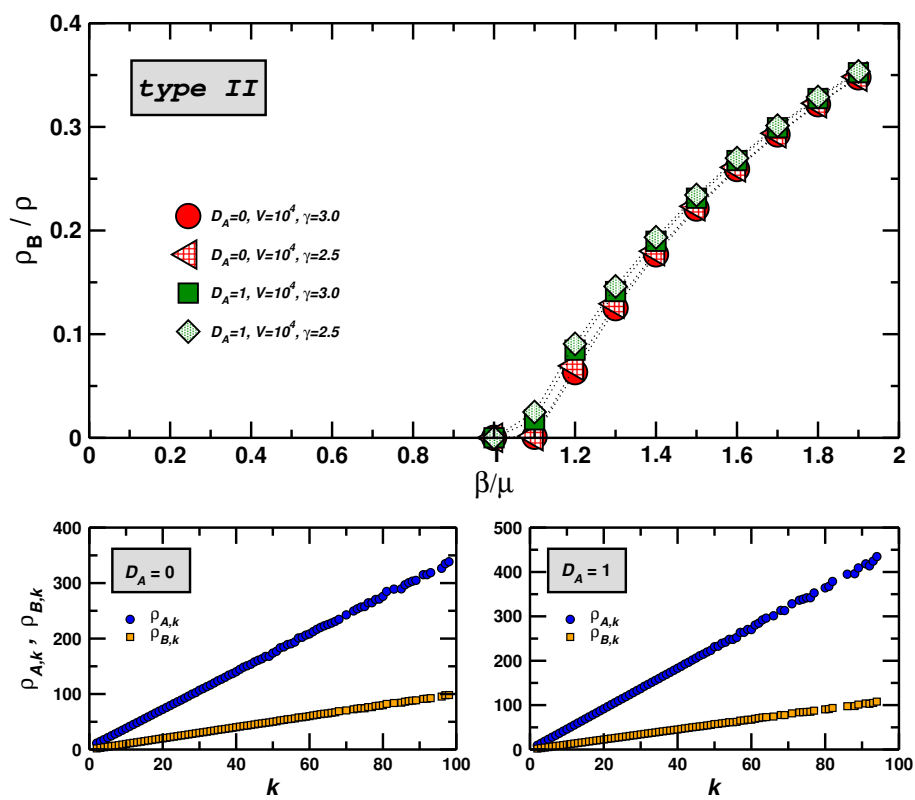


Figure 3.

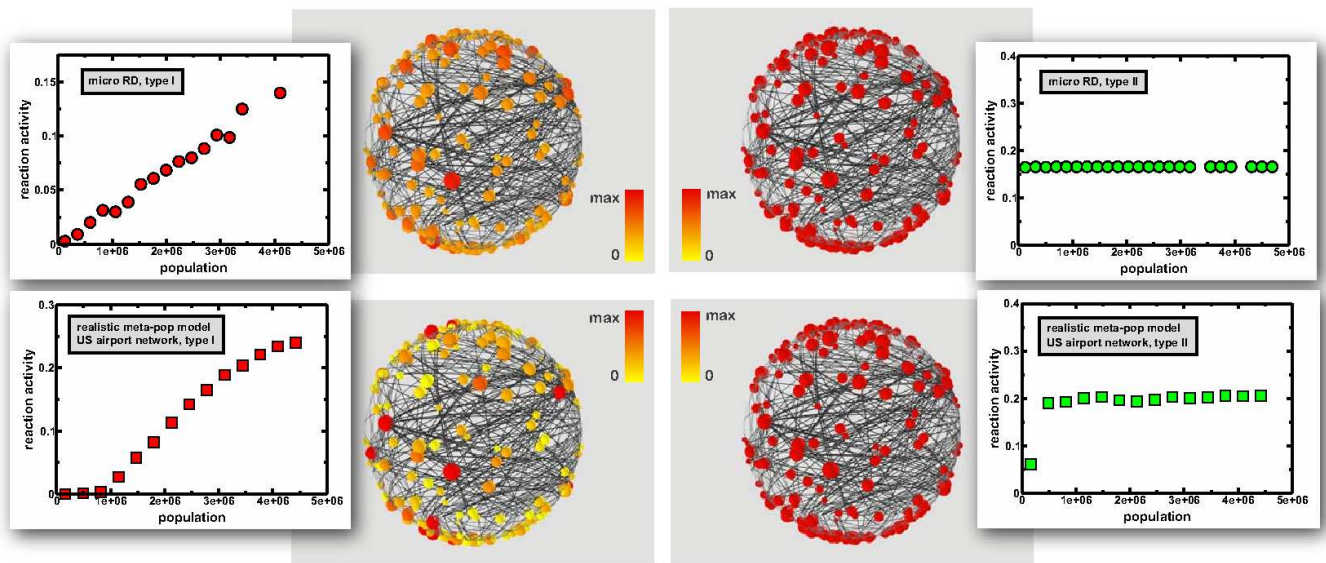


Figure 4.